Analyses of repair and maintenance of a masonry wall

G.C.Beolchini**, F.Grillo* & G.Valente**
(*) Dipartimento di Ingegneria Strutturale e Geotecnica, Università di Roma "La Sapienza".
(**) Dipartimento di Ingegneria delle Strutture Acque e Terreno, Università de L'Aquila.
EMail: valente@disat.ing.univaq.it

Abstract

For the masonry walls, we use low tensile strength and fracture energy. The nonlinear uniaxial compressive behaviour is defined by initial Young's modulus E, crushing point and ultimate point in the stress-strain plane. In multiaxial compressive stress condition, the crushing and ultimate points may be enhanced, relating to the projection on the multiaxial failure envelope in principal stress axes. Unloading from a compressive state is parallel to the initial Young's modulus. Cracking occurs when one tensile principal stress tends to overcome the tensile strength. A crack plane develops at right angle to the previous principal direction and is conserved its orientation for the whole loading process. Subsequent crack planes could be only orthogonal to the first and between them. After cracking, the stiffness matrix at the integration point is modified according to fracture or aggregate interlock theories. The local tangent stiffness matrix is referred to: 1) principal stress directions before tensile failure, 2) cracks coordinate system after tensile failure. The convergence tolerances on unbalanced load and energy are imposed within 0.1%. Initially, masonry panels were obtained by the wall and were tested "in situ" in compression, splitting and shear tests. These three experimental tests were compared with analogous numerical analyses in order to obtain all the mechanical characteristics for the wall analysis. Cyclic tests on a stone wall of irregular size for a building placed in l'Aquila were performed. These tests were compared with analogous analyses, both to design the tests and to obtain new mechanical features of the material. The damaged wall were strengthened with various steel reinforcements, and then analyzed with new load conditions.

1 Introduction

In this paper the computed results obtained by a general purpose code like ADINA, used to define the numerical behaviour of old stone masonries, are presented and discussed. The analysis was performed by comparing numerical results with experimental data obtained by compression and diagonal compression tests on panels square shaped about 1.0 by 1.0 m as in Fig.1; the identified parameters were used to predict the experimental behaviour of a wall about 5.0 m height, loaded in its plane by fully reversed cyclic forces.

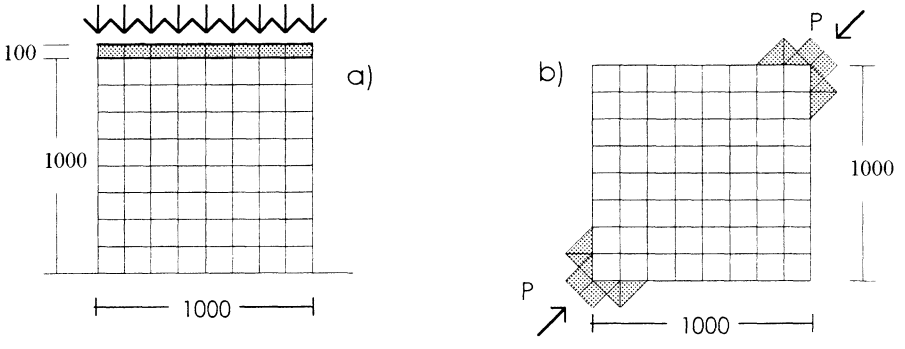

Figure 1: Models for the tests: a) compressive, b) diagonal compressive.

Then, this wall was tested experimentally. And the same wall, already damaged, strengthened with two different reinforcements is presented here.

2 Rough crack model

The significance of this effect was brought to light by recent experimental results, which also revealed that the phenomenon of shear transfer accross a crack is highly nonlinear.

The experimental data presently available [6] made it possible to develop some much realistic models.

The stresses σ_{nn} (always compressive) and σ_{nt} as functions of δ_n and δ_t are used according to the model proposed by Bazant and Gambarova [6], with constant values $\tau_0=\eta_s\ \sigma_c$; these two function are shown in Fig.2, with the variation intervals of all the variables.

Some properties of the model are:

1. The existence of singularity calls for imposing an energy restriction. The work consumed or released by the crack as the displacements increase from zero to any δ_n and δ_t must be bounded, i.e.

$$-\infty < W=\int\sigma_{nn}\, d\delta_n + \int\sigma_{nt}\, d\delta_t < +\infty \qquad (1)$$

the sign of the frictional stress σ_{nt} is the same as for the slip δ_t. The work condition in Eq.1 restricts the admissible loading paths in the (δ_n, δ_t) plane. The admissible path may be approximated near the origin by the equation :

$$\delta_t = c\,\delta_n^a \tag{2}$$

where c,a are positive constants with a>1. This indicates that

$$d\delta_t/d\delta_n = 0 \qquad \text{for } \delta_n = 0 \tag{3}$$

2. The normal and shear stiffness of cracked concrete could never exceed the analogous coefficients of undamaged concrete

$$B_{nn}\, w < E, \quad B_{tt}\, w < G \tag{4}$$

3. The following limits must be observed:

$$\sigma_1 = (\sigma_{nn}/2) + \sqrt{[(\sigma_{nn}/2)^2 + \sigma_{nt}^2]} < \sigma_t, \qquad \sigma_2 = (\sigma_{nn}/2) - \sqrt{[(\sigma_{nn}/2)^2 + \sigma_{nt}^2]} > \sigma_c,$$
$$\sigma_{nt} < \tau_0 \tag{5}$$

The equations 1.,3.,4.,5. produce the boundary of feasible domain as in Eq.(2).

From the two functions σ_{nn} , σ_{nt} , the partial derivatives $B_{tt} = \partial\sigma_{nt}/\partial\delta_t$, $B_{tn} = \partial\sigma_{nt}/\partial\delta_n$, $B_{nt} = \partial\sigma_{nn}/\partial\delta_t$, $B_{nn} = \partial\sigma_{nn}/\partial\delta_n$ are obtained for the stiffness matrix.

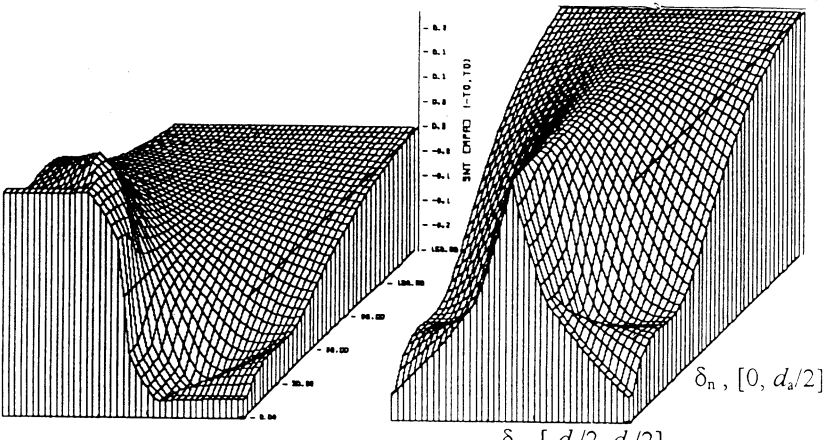

Figure 2a: Func.$\sigma_{nt}(\delta_n, \delta_t)$, $[-\tau_0, \tau_0]$,. Figure 2b: Func.$\sigma_{nn}(\delta_n, \delta_t)$, $[\sigma_c, 0]$

3 Nonlocal strains

The nonlocal strains are evaluated for the strain-softening branch alone, while the elastic strains $\varepsilon_i(s) = \sigma_t/E_0$, are local everytime, see paper [6].

If the concrete is damaged in V, the full nonlocal strain tensor is evaluated by spatial averaging as follows [6]:

$$\underline{\varepsilon}(x) = \int \alpha'(x,s)\,[\varepsilon(s) - \varepsilon_i(s)]\,dV \tag{5}$$

in which:

$$\alpha'(x,s) = \alpha(s-x)/V_r(x), \qquad V_r(x) = \int \alpha(s-x)\,dV, \tag{6}$$

x = point coordinates in which nonlocal strains are evaluated.
s = point coordinates in volume V.
$\underline{\varepsilon}$, ε = nonlocal and local strains; (the nonlocal tensor is underscored);
$\varepsilon = [\varepsilon_x \varepsilon_y \varepsilon_z \gamma_{xy} \gamma_{yz} \gamma_{zx}]$ the full strain tensors
$\varepsilon_i(s) = \sigma_t/E_0$ elastic strain
V=volume of the entire body, centered in x with radius w.

The square brackets [] denote the damaged concrete; i.e. $[\varepsilon(s)-\varepsilon_i(s)]>0$ for cracked concrete, and $[\varepsilon(s)-\varepsilon_i(s)]=0$ for undamaged concrete. It has experienced that the calculation converges better if $\alpha(x)$is the Gaussian distribution function:

$$\alpha(x)=\exp\,[-(k\,x/w)^2] \qquad (k=2 \text{ for 2D problems}) \qquad (7)$$

From the full nonlocal strain, the crack opening and crack slip are obtained:

$$\delta_n = w\,\underline{\varepsilon}_{nn}, \qquad \delta_t = w\,\underline{\gamma}_{nt} \qquad (8)$$

The wall damage is spreaded along the characteristic length depending on the maximum aggregate size d_a; this length influences all the parameters of the analysis and is fixed equal to a $w = 3d_a = 900.$ mm.

Both fracture and aggregate interlock are analyzed with nonlocal strains, through the parameters: $\underline{\delta}_n$, $\underline{\delta}_t$, B_{tt}, B_{tn}, B_{nt}, B_{nn} [6]. In this way, the results are not sensitive to the dimension and to the slope of the mesh, but are depending on the characteristic length w alone.

4 Panels subjected to compression with E=200.÷500. MPa

The experimental results are quite scattered. The average experimental mechanical features, obtained by Beolchini et al. [4], are shown in Table I at the first row. In the same Table, the analogous mechanical features adopted for the analysis, are shown. Referring to uniaxial tests: E_0 is the initial tangent elasticity modulus, σ_c and σ_u are the maximum and the ultimate compressive stresses, ε_c and ε_u are the corresponding strains; ν is the Poisson's coefficient, K is the secant modulus for $\sigma = \sigma_c/3$, η_s =0.20 is the friction coefficient.

Table I - Mechanical features of the masonry.

	E_0	$K(\sigma_c/3)$	σ_c	ε_c	σ_u	ε_u	ν
Exper.	166.8		-1.02	-.00992	-1.00	-.01110	
CODE	200.0	161.5	-1.02	-.00992	-0.99	-.0114	0.20
CODE	500.0	323.	-1.02	-.005	-0.99	-.0057	0.20
	MPa	MPa	MPa			MPa	

The experimental tests, performed by Beolchini et al. [2] and [3], arrived to a maximum trasversal strain $\varepsilon = 0.006$, higher than numerical analogous.

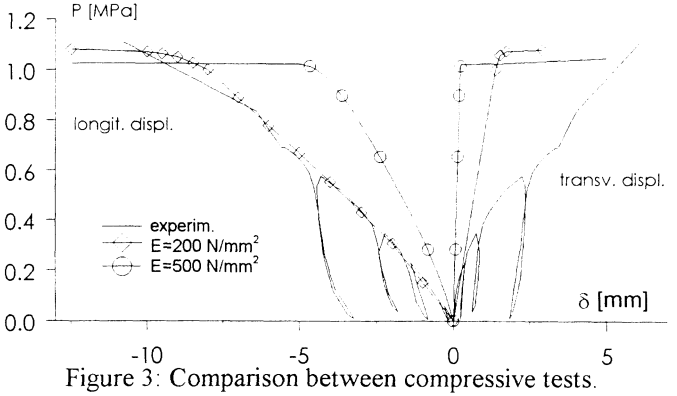

Figure 3: Comparison between compressive tests.

5 Panels subjected to diagonal compression, E=200÷500 Mpa

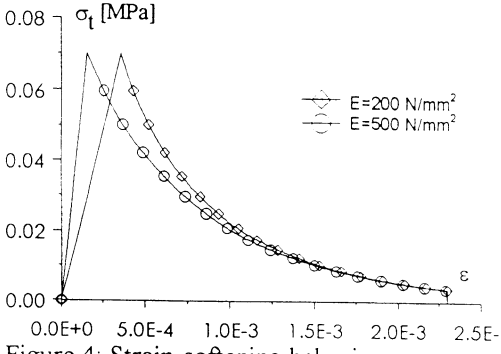

Figure 4: Strain-softening behaviour.

The maximum aggregate size was d_a =300.mm. The assumed mechanical features for the ana lysis were: fracture energy G_F = 0.055 N/mm, tensile stren gth σ_t=.07 MPa, characteristic length $w = 3\ d_a$. The strain-softening behaviour was assu med exponential, truncated for tensile stress σ<0.05 σ_t, accor- ding to micromechanic analysis by Bazant of 1987, as in Fig.4.

In Fig. 5a, the experimental and analytical curves P-δ for diagonal compressive tests are compared. It may be noted that the analytical curves P-δ for compressive diagonal is more stiff then experimental one

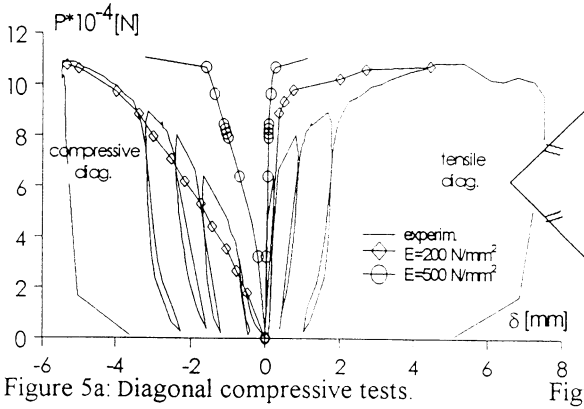

Figure 5a: Diagonal compressive tests.

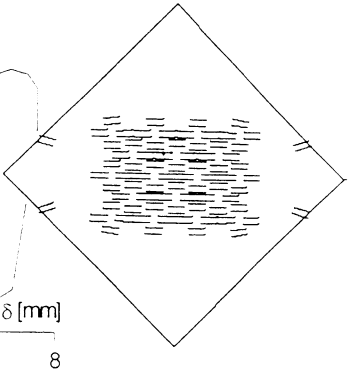
Figure 5b: Max. crack field.

The experimental results for the masonry panels show a better fitting with analogous experimental with initial tangent elasticity modulus E_0 =200. Mpa.

Instead, the experimental results for the walls show a better fitting with analogous experimental for an initial tangent elasticity modulus E_0 =500. Mpa.

6 Reinforced panels subjected to diagonal compression

The same masonry panels were strengthened with two bars having diameter ∅=12 mm, and then subjected to diagonal compression, as in Fig.6.

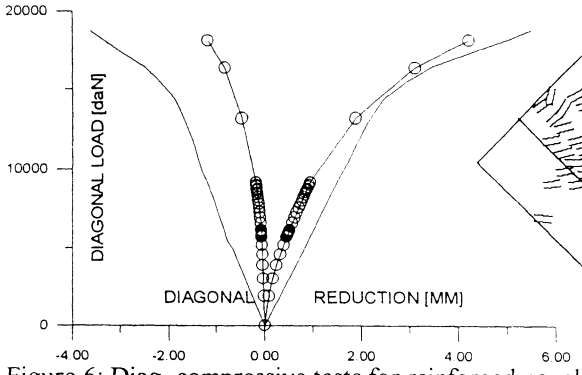

Figure 6: Diag. compressive tests for reinforced panel; (---) experimental, (ooo) numerical with E=500 Mpa.

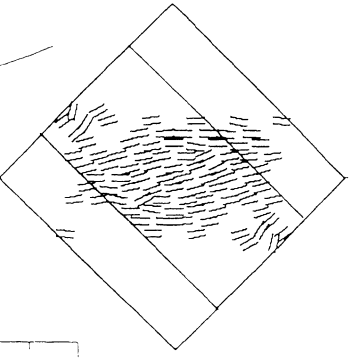

Figure 6b: Max.crack field for E=500. MPa.

7 Unreinforced wall loaded at the 2.nd floor

The wall studied in this paper was isolated in a building (see Figure 7a) destined to demolition; two horizontal slabs were built in reinforced concrete in order to better distribute the applied loads, for static and dynamic tests, up to damaging also. The test modes were shown by Vestroni et al., [7]. The wall was firstly analyzed with the initial tangent elasticity modulus E_0 =200. Mpa obtained by comparison with experimental results for the panels; these analytical results were published by Beolchini et al. [5]. Then, the same masonry wall was tested.

For the masonry wall, the comparison of the experimental curves P-δ with the analogous analytical obtained by assuming E_0 =200. Mpa [8], showed:

a) the initial experimental stiffness of the wall was higher, attainable analitycally with E_0 =500. Mpa

b) the experimental ductility was higher, not attainable analitycally for insuperable problems for the equilibrium iterations.

The scheme of the masonry wall and the load conditions are shown in Fig. 7.

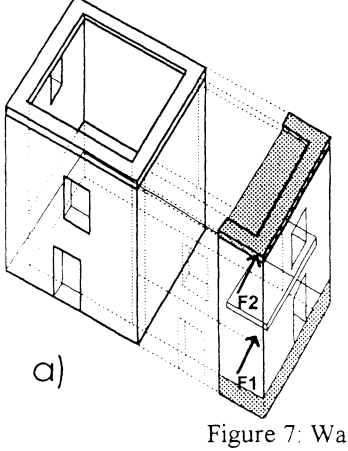

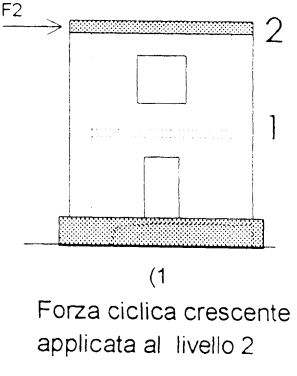

Figure 7: Wall scheme and load conditions.

All the masonry meshes, both for the panels and for the walls, were considered in plane stress condition.

In Fig. 8a the experimental and numerical curves P-δ are compared.

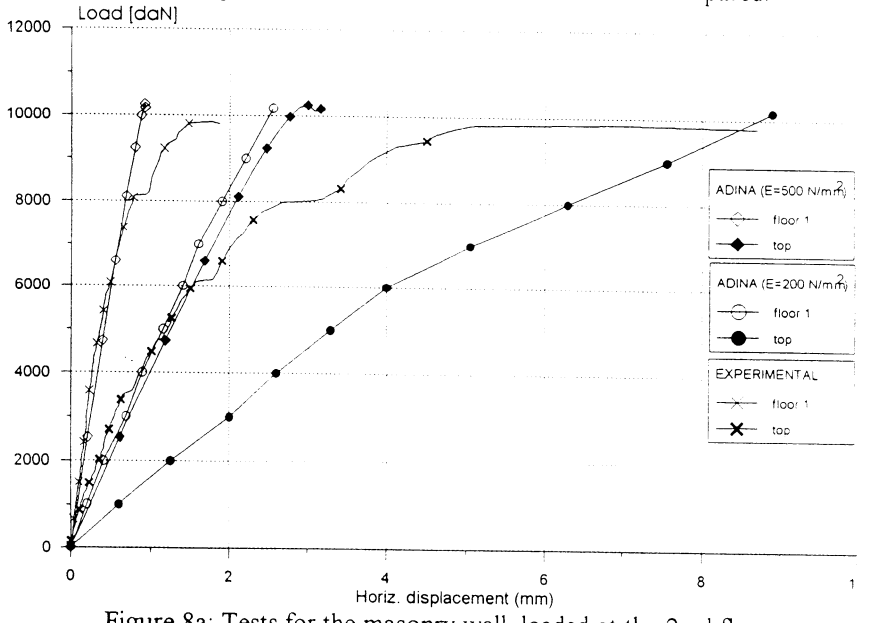

Figure 8a: Tests for the masonry wall, loaded at the 2.nd floor.

The Authors consider more reliable the initial tangent elasticity modulus E_0 =500 Mpa obtained by comparison on masonry walls for the following reasons: the maximum aggregate size was d_a =300.mm. For the panel the ratio between its side and the maximum aggregate size was about 3, too small to obtain significant experimental resul ts, instead for the wall the same ratio was about 16.

Then, all the subsequent wall analyses were performed with E_0 =500. Mpa.

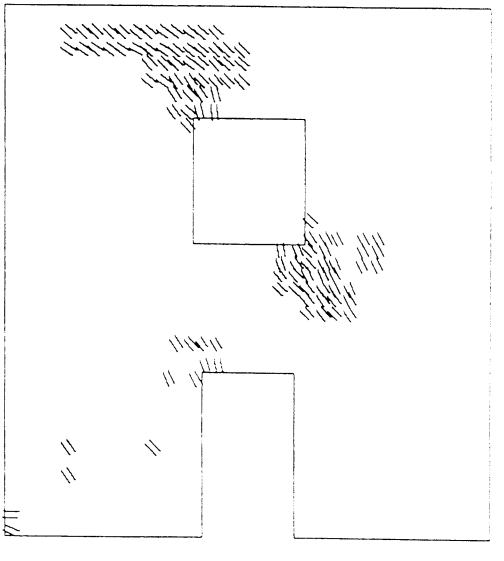

Figure 8b: Max crack field for E=500 MPa.

8 Unreinforced wall loaded at both the floors

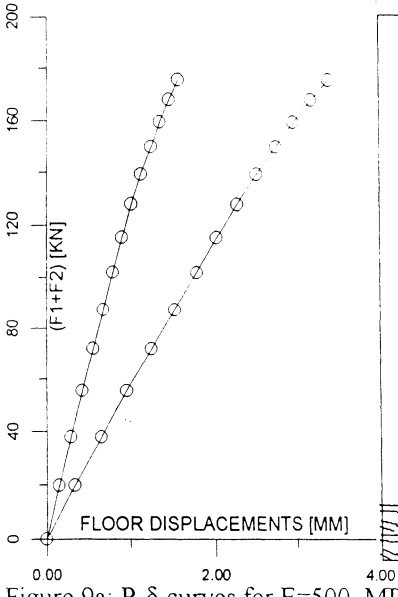

Figure 9a: P-δ curves for E=500. MPa.

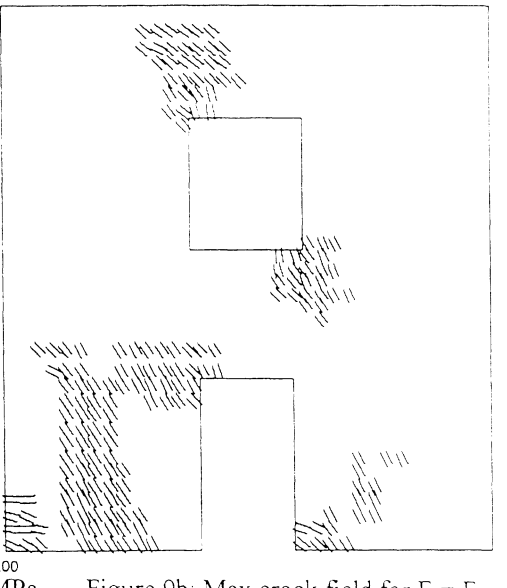

Figure 9b: Max.crack field for $F_1 = F_2$.

9 Reinforced wall

The original damaged wall was analyzed strengthened with horizontal steel bars having diameter ∅=12 mm: 2 on the left and 2 on the right of the door and of the window, for the total of 8 bars, at 1/4 of the height of the openings, for all the width of the wall.

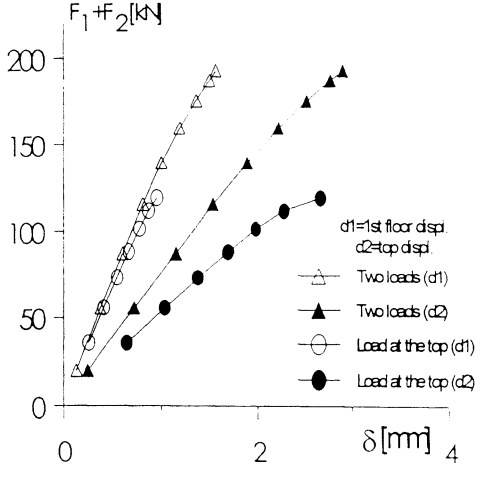

Figure 10a: P-δ curves for E=500. Mpa.

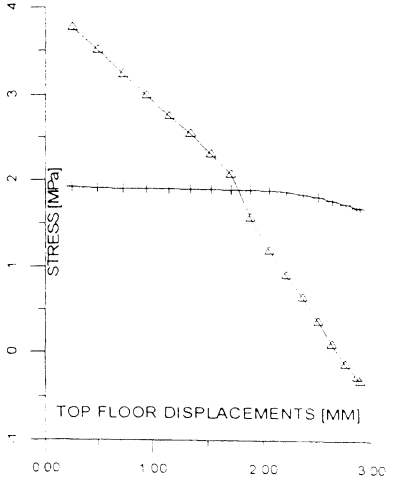

Figure 10b: Steel stresses for $F_1 = F_2$ (+++)window reinf., (ΔΔΔ)door r

10 Prestressed wall

The original damaged wall was analyzed strengthened with prestressing reinforcements:

a) vertically to produce a stress increment of 0.1 MPa in the two walls, on the left and on the right of the door, with A=2828.mmq at each side.

b) horizzontally to produce a stress increment of 0.2 Mpa, in the masonry at the level of the first floor, with A=2813. mmq; from Fig.11b, this last prestressing seems insignificant.

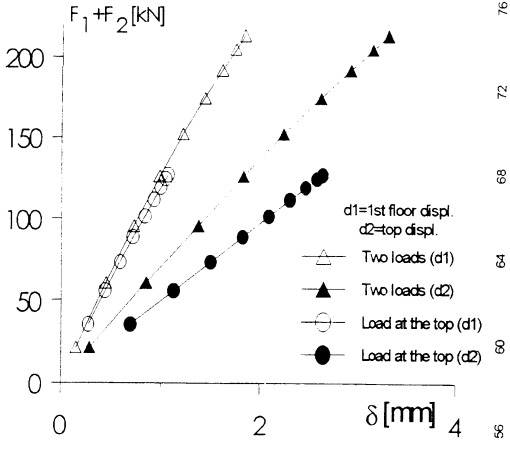

Figure 11a: P-δ curves for E=500. Mpa.

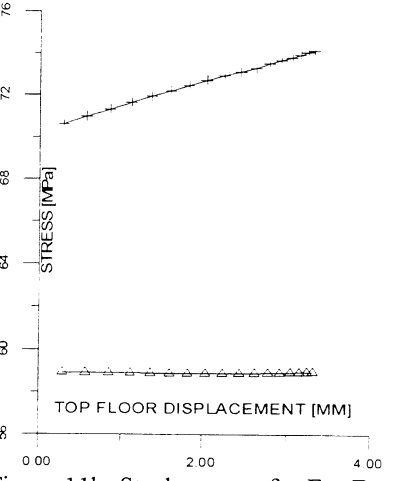

Figure 11b: Steel stresses for $F_1 = F_2$ (+++)vertical left, (ΔΔΔ)horizontal.

11 Conclusions

The analyses showed that the proposed Code could be used successfully for the study of the behaviour of masonry structures.

By the comparison between experimental and numerical curves P-δ, the mechanical features of the masonry were obtained:

a) the stresses and the strains at crushing and ultimate and Poisson's ratio by the compression on the panels;

b) the tensile strength, the fracture energy and the strain-softening behaviour by diagonal compression on the panels;

c) the initial tangent elaticity modulus and the friction coefficient by the walls.

The analysis results are satisfactory for the initial shape of the curves P-δ, for the crack field, for the ultimate loads; the ultimate displacements by the tests are higher than numerical for insuperable problems of the equilibrium iterations.

This Code seemed promising; for this reason, the original damaged masonry wall was analyzed strengthened with horizontal steel reinforcements, or with prestressing reinforcements.

In the following Table II are shown the ultimate loads for unreinforced, reinforced and prestressed masonry walls, for the two load conditions; the

increases for reinforced wall are insignificant, instead for prestressed wall are about 20%.

Table II: Ultimate loads of the walls for two load conditions.

Masonry	unreinforced	reinforced	prestressed
a) load at the top, F_1=0, F_2=	102.4	109.2	127.1
b) two loads F_1= F_2=	91.7	96.6	109.2
	KN	KN	KN

Acknowledgements

This paper was supported by the following grants: CNR-GNDT, Ct. 96.02935.PF54 e MURST 60% 1995.

References

1. Beolchini, G.C., Capecchi, D., Grillo F. & Vestroni F. La Casa di Porta Bazzano in L'Aquila-Sperimentazione su un Vecchio Edificio in Muratura, *Atti DISAT*, 1989, n.21.
2. Beolchini G.C., Grillo F., 1989b. Prove Statiche su Pannelli Murari di un Edificio Aquilano del '700, pp.770-782, Vol.2, *Proceedings of the 4th Convegno Nazionale "L'Ingegneria Sismica in Italia"*, Milano, 1989.
3. Beolchini, G.C. & Grillo F. In Situ Tests of Stone Masonry Panels, pp.178-187, Vol.6, *Proceedings of IX ECEE*, Moscow, 1990.
4. Beolchini, G.C. & Grillo, F. La Normativa Italiana e le Vecchie Costruzioni Abruzzesi in Muratura di Pietrame, pp.1253-1262, Vol.2, *Proceedings of the 5th Convegno Nazionale Ingegneria Sismica in Italia,* Palermo, 1991.
5. Beolchini, G., Gavarini, C., Grillo, F., Mollaioli, F. & Valente, G. Analisi Preventiva per le Prove sulla Parete in Muratura di un Edificio, pp. 425-434, *Proceedings of the 7th Convegno Nazionale Ingegneria Sismica in Italia,* Siena, 1995.
6. Valente, G. Modelling of Crack Shear in Concrete, *Proceedings of EURO-C,* Innsbruck, 1994.
7. Vestroni, F., Beolchini, G., Grillo, F., Martinelli, A., Ricciardulli, G.L. & Buffarini, G., 1995. Il Progetto di un'Indagine Sperimentale su una vecchia Casa in Muratura, pp. 331-340, *Proceedings of the 7th Convegno Nazionale Ingegneria Sismica in Italia*, Siena, 1995
8. Beolchini, G., Grillo, F. & Valente, G. La modellazione numerica del comportamento di una muratura in pietrame, *Proceedings of the Convegno "La Meccanica delle Murature tra Teoria e Progetto"*, Messina, 1996.